1521-0111/100/1/19–31$35.00
https://doi.org/10.1124/molpharm.121.000268
Molecular Pharmacology
Mol Pharmacol 100:19–31, July 2021

Intrasubunit and Intersubunit Steroid Binding Sites Independently and Additively Mediate $\alpha1\beta2\gamma2$L $GABA_A$ Receptor Potentiation by the Endogenous Neurosteroid Allopregnanolone[S]

Allison L. Germann, Spencer R. Pierce, Hiroki Tateiwa, Yusuke Sugasawa, David E. Reichert, Alex S. Evers, Joe Henry Steinbach, and Gustav Akk

Departments of Anesthesiology (A.L.G., S.R.P., H.T., A.S.E., J.H.S., G.A.) and Radiology (D.E.R.), and the Taylor Family Institute for Innovative Psychiatric Research (D.E.R., A.S.E., J.H.S., G.A.), Washington University School of Medicine, St. Louis, Missouri; and Department of Anesthesiology and Pain Medicine, Juntendo University School of Medicine, Tokyo, Japan (Y.S.)

Received February 21, 2021; accepted April 22, 2021

ABSTRACT

Prior work employing functional analysis, photolabeling, and X-ray crystallography have identified three distinct binding sites for potentiating steroids in the heteromeric $GABA_A$ receptor. The sites are located in the membrane-spanning domains of the receptor at the β-α subunit interface (site I) and within the α (site II) and β subunits (site III). Here, we have investigated the effects of mutations to these sites on potentiation of the rat $\alpha1\beta2\gamma2$L $GABA_A$ receptor by the endogenous neurosteroid allopregnanolone (3α5αP). The mutations were introduced alone or in combination to probe the additivity of effects. We show that the effects of amino acid substitutions in sites I and II are energetically additive, indicating independence of the actions of the two steroid binding sites. In site III, none of the mutations tested reduced potentiation by 3α5αP, nor did a mutation in site III modify the effects of mutations in sites I or II. We infer that the binding sites for 3α5αP act independently. The independence of steroid action at each site is supported by photolabeling data showing that mutations in either site I or site II selectively change steroid orientation in the mutated site without affecting labeling at the unmutated site. The findings are discussed in the context of linking energetic additivity to empirical changes in receptor function and ligand binding.

SIGNIFICANCE STATEMENT

Prior work has identified three distinct binding sites for potentiating steroids in the heteromeric γ-aminobutyric acid type A receptor. This study shows that the sites act independently and additively in the presence of the steroid allopregnanolone and provide estimates of energetic contributions made by steroid binding to each site.

Introduction

The γ-aminobutyric acid type A ($GABA_A$) receptor is the major ionotropic transmitter-gated inhibitory ion channel in the brain. It normally responds to synaptically released or ambient GABA, but a large number of endogenous and clinical compounds, including neurosteroids, benzodiazepines, and several intravenous anesthetics can activate the receptor and/or modulate its response to the transmitter. Endogenous neurosteroids and their synthetic analogs exhibit a large range of efficacies on the $GABA_A$ receptor (Park-Chung et al., 1999; Li et al., 2007a). Steroids have an apparent affinity to the receptor in the micromolar range, although the actual K_Ds may be several log-orders higher because of accumulation of steroid in the lipid bilayer (Akk et al., 2005; Li et al., 2007b).

Functional analysis, photolabeling, and X-ray crystallography have identified three distinct binding sites for potentiating steroids in the membrane-spanning domains of the heteromeric $GABA_A$ receptor (Hosie et al., 2006; Laverty et al., 2017; Miller et al., 2017; Ziemba et al., 2018; Chen et al., 2019). The sites are located at the β-α subunit interface (dubbed site I) and within the α (site II) and β subunits (site III) (Fig. 1). Site I is the canonical binding site located in the cleft between the β subunit "+" and the α subunit "-" surfaces. The steroid positions with its A-ring oriented toward the

This work was supported by National Institutes of Health National Institute of General Medical Sciences [Grant R01GM108580] and [Grant R01GM108799] and funds from the Taylor Family Institute for Innovative Psychiatric Research.
The authors have no financial conflicts of interest.
Primary laboratory of origin: Department of Anesthesiology, Washington University School of Medicine, St. Louis, MO.
http://doi.org/10.1124/molpharm.120.000268.
[S] This article has supplemental material available at molpharm.aspetjournals.org.

ABBREVIATIONS: 3α5αP, 1-[(3R,5S,8R,9S,10S,13S,14S,17S)-3-hydroxy-10,13-dimethyl-2,3,4,5,6,7,8,9,11,12,14,15,16,17-tetradecahydro-1*H*-cyclopenta[*a*]phenanthren-17-yl]ethanone (allopregnanolone); DDM, *n*-dodecyl-β-D-maltoside; DTT, dithiothreitol; ELIC, *Erwinia* ligand-gated ion channel; $GABA_A$, γ-aminobutyric acid type A; KK200, (3α,5α,17β)-17-[[4-[3-(trifluoromethyl)-3*H*-diazirin-3-yl] phenyl] methoxy]-androstane-3-ol; MBP, maltose binding protein; MS, mass spectrometry; PA, probability of being in the active state; PR, probability of being in the resting state; TM, membrane-spanning segment; TMD, transmembrane domain.

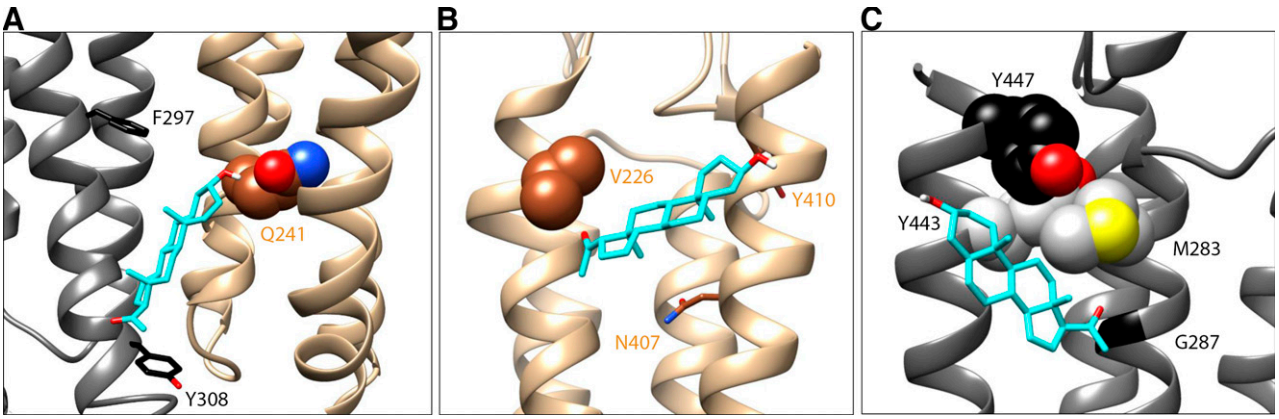

Fig. 1. Docking of 3α5αP in the putative binding sites. The panels show side views of the putative β-α intersubunit binding site (site I; A), the intra-α subunit site (site II; B), and the intra-β subunit site (site III; C). The α subunit is shown in tan, the β subunit in gray. 3α5αP (cyan) is docked in each site. In site I, the Q241 residue in α1TM1 is shown as a sphere. Residues homologous to Y308 (Y309) and F297 (F298) in TM3 are photolabeled by KK200 in ELIC-α1 and ELIC-α1(Q242L), respectively, and are shown as ball & stick. In site II, the V226 residue in αTM1 is shown as a sphere. The N407 and Y410 residues in αTM4 previously identified to contribute to steroid binding are shown as ball & stick. In site III, the M283 (light gray; βTM3), Y443 (light gray; βTM4), and Y447 (black; βTM4) are shown as sphere. The G287 residue in βTM3 is identified as black ribbon.

hydrophobic core of the membrane facing the α(Q241) residue in the first membrane-spanning segment (TM 1), and the D-ring near the β(F301) residue in TM3 pointing toward the cytoplasmic side of the membrane. Site II is within a cavity between the extracellular ends of the TM1 and TM4 segments of the α subunit. The A-ring of the steroid is proximal to the α(Y415) residue at the extracellular side of the membrane, and the D-ring is positioned near the α(N407) residue. In TM1, the steroid abuts the α(V226) residue. Site III is located between the TM3 and TM4 segments of the β subunit. The A-ring of the steroid is positioned toward the extracellular domain near the β(Y443) residue in TM4 and the D-ring near β(G287) of TM3.

Mutations introduced to sites I [e.g., α1(Q241L) and αQ(241S)] and II [e.g., α1(V226W)] reduce receptor potentiation by allopregnanolone (3α5αP) and other potentiating steroids thus demonstrating the functionality of these binding sites (Hosie et al., 2006; Akk et al., 2008; Chen et al., 2019). In contrast, no change in potentiation by 3α5αP or pregnanolone was observed in a recent study probing the effects of amino acid substitutions at a limited set of residues in site III in the α1β3 $GABA_A$ receptor (Chen et al., 2019).

The existence of several distinct sites in the relatively compact transmembrane regions of the receptor raises the possibility that the sites interact directly with each other by some form of conformational coupling. Here, we have investigated the effects of mutations to these three steroid binding sites on potentiation of the α1β2γ2L $GABA_A$ receptor by the endogenous steroid 3α5αP. The mutations were introduced alone or in combination to probe the additivity of effects. We show that the effects of amino acid substitutions in sites I and II are energetically additive, indicating independence of steroid actions at the two binding sites. We also used neurosteroid analog photolabeling to show that mutations in either site I or site II selectively affect steroid orientation and efficacy of labeling only in the mutated site, supporting the absence of allosteric interaction between the sites. In site III, none of the mutations tested reduced potentiation by 3α5αP. The findings are discussed in the context of linking energetic additivity to empirical changes in receptor function and ligand binding.

Materials and Methods

Receptor Expression and Electrophysiological Recordings. The rat α1β2γ2L $GABA_A$ receptors were expressed in oocytes from *Xenopus laevis* (African clawed frog). Quarter ovaries were purchased from Xenoocyte (Dexter, MI), and digested at 37°C with shaking at 250 RPM for 15–30 minutes in 2% w/v (mg/mL) collagenase A solution in ND96(96 mM NaCl, 2 mM KCl, 1.8 mM $CaCl_2$, 1 mM $MgCl_2$, 5 mM HEPES; pH 7.4) with 100 U/ml penicillin and 100 μg/ml streptomycin. After digestion, the oocytes were rinsed in ND96 and stored in ND96 with supplements (2.5 mM Na pyruvate, 100 U/ml penicillin, 100 μg/ml streptomycin, 50 μg/ml gentamycin) at 15°C for at least 4 hours before injection.

The cDNAs for rat α1 (GenBank accession number NM_183326), β2 (NM_012957), and γ2L (NM_183327) subunits in the pcDNA3 vector were linearized with XbaI (NEB Laboratories, Ipswich, MA). The following mutant clones, generated using QuikChange (Agilent Technologies, Santa Clara, CA), were studied: α1(Q241L), α1(Q241S), α1(V226W), α1(Q241L + V226W), α1(Q241S + V226W), β2(M283A), β2(G287W), β2(Y443W), and β2(Y447A). The clones were fully sequenced prior to use. The complementary RNAs were generated from linearized cDNA using Message Machine (Ambion, Austin, TX).

The oocytes were injected with a total of 3.5 ng of complementary RNA per oocyte, in the ratio of 1:1:5 (α1:β2:γ2L) to enhance expression and incorporation of the γ2L subunit. After injection, the oocytes were incubated in ND96 with supplements (2.5 mM Na pyruvate, 100 U/ml penicillin, 100 μg/ml streptomycin, and 50 μg/ml gentamycin) at 15°C for 1 to 2 days prior to conducting electrophysiological recordings.

The electrophysiological recordings were performed using standard two-electrode voltage clamp. The oocytes were clamped at −60 mV. Bath and drug (GABA, steroids, propofol) solutions were gravity-applied from glass syringes with glass luer slips via Teflon tubing to the recording chamber (RC-1Z, Warner Instruments, Hamden, CT) at a flow rate of 6–8 ml/min. Solutions were switched manually using 4-port bulkhead switching valve and medium-pressure 6-port bulkhead valves (IDEX Health and Science, Rohnert Park, CA). All experiments were conducted at room temperature.

GABA concentration-response curves were measured by exposing cells expressing GABA$_A$ receptors to 1, 3, 10, 30, 100, 300, and 1000 μM GABA. 3α5αP concentration-response curves were measured by exposing cells to a low concentration of GABA alone, and in the presence of 0.01, 0.03, 0.1, 0.3, 1, 3, and 10 μM steroid. The drug applications lasted 20–80 seconds and were aimed at determining the amplitude of the peak response. Successive drug applications were separated by >1-minute washouts in ND96. Each cell was exposed to the full range of GABA or steroid concentrations. Some experiments were conducted by measuring the effect of a steroid on steady-state activity elicited by a low concentration of GABA.

The current responses were amplified with an OC-725C amplifier (Warner Instruments, Hamden, CT), digitized with a Digidata 1200 series digitizer (Molecular Devices), and stored using pClamp (Molecular Devices). The current traces were analyzed using Clampfit (Molecular Devices).

Analysis of Electrophysiological Data. GABA concentration-response curves were fitted, separately for each cell, to the Hill equation using raw current amplitudes. 3α5αP concentration-response data were first converted to units of probability of being in the active state (P_A units) through normalization to the peak response to saturating (1 mM) GABA + 50 μM propofol, that was considered to have a peak P_A indistinguishable from 1 (Shin et al., 2017). The probability of constitutive activity in the absence of any applied agonist was determined by comparing the response amplitudes to 100 μM picrotoxin and 1 mM GABA + 50 μM propofol. The level of constitutive activity was negligible (< 0.003) for all receptors used and was thus not included in the calculation of P_A.

The peak current responses expressed in P_A units were then analyzed using a cyclic two-state concerted transition model (Steinbach and Akk, 2019). The 3α5αP concentration-response curves were fitted, separately for each cell, to the state function:

$$P_{A,\,peak} = \frac{1}{1 + L^* \left[\frac{1+[3\alpha5\alpha P]/K_{R,\,3\alpha5\alpha P}}{1+[3\alpha5\alpha P]/(K_{R,\,3\alpha5\alpha P} c_{3\alpha5\alpha P})}\right]^N} \quad (1)$$

where L* expresses the level of background activity in the presence of a low concentration of GABA, and can be calculated as $(1 - P_{A,GABA})/P_{A,GABA}$. $K_{R,3\alpha5\alpha P}$ is the equilibrium dissociation constant for 3α5αP in the resting receptor, $c_{3\alpha5\alpha P}$ is the ratio of the equilibrium dissociation constant for the steroid in the active receptor to $K_{R,3\alpha5\alpha P}$, and [3α5αP] is the concentration of the steroid. $N_{3\alpha5\alpha P}$, the number of binding sites for 3α5αP, was constrained to 2 in the initial analysis.

Curve fitting was done using Origin 2020 (OriginLab Corp., Northampton, MA) with L*, $K_{R,3\alpha5\alpha P}$, and $c_{3\alpha5\alpha P}$ as free parameters. Statistical analyses were done using Excel 2016 (Microsoft, Redmond, WA). Steroid-induced potentiation is calculated as ratio of peak responses in the presence and absence of steroid (1 = no effect). The results are reported as mean ± S.D. from at least 5 cells for each experiment. All data are included in analysis. The study is exploratory by nature. The findings are reported according to the guidelines detailed in (Michel et al., 2020).

ELIC-α1 Construct Design. The ELIC-α1 GABA$_A$ receptor chimera was constructed by fusing the extracellular domain of ELIC (*Erwinia* ligand-gated ion channel) to the transmembrane domain (TMD) of human α1 subunit of the GABA$_A$ receptor (Kinde et al., 2016; Chen et al., 2018; Sugasawa et al., 2019). The intracellular loop amino acids were substituted by the short linker -GVE- sequence. A decahistidine tag and a maltose binding protein (MBP) were incorporated at the amino-terminal, and a tobacco etch virus protease cleavage site was inserted between MBP and ELIC-α_1 GABA$_A$ receptor (Chen et al., 2018; Sugasawa et al., 2019).

Expression and Purification. Mutagenesis was performed as described previously (Kinde et al., 2016; Chen et al., 2018; Sugasawa et al., 2019) by oligonucleotide-directed mutagenesis using *Phu* polymerase (Thermo Fisher Scientific) verified by sequencing. The ELIC-α1 GABA$_A$ receptor was expressed in OverExpress C43(D3) *E. coli*, derived from Rosetta (DE3) cells under double selection with kanamycin (50 μg/mL) and chloramphenicol (10 μg/mL). A few isolated colonies were used to inoculate 100 mL of LB (Sigma-Aldrich) media with the antibiotics and grown overnight at 37°C in a shaker at 250 rpm. The overnight culture was then diluted 1:100 into 6 × 1 liters of LB media with antibiotics and grown to an optical density of 0.7–0.8. All six liters were harvested (5000 rpm, 15 minutes, 4°C) and resuspended in 2 liters of LB media supplemented with 0.5 M sorbitol. The concentrated cells were equilibrated in a shaker at 15°C and 250 rpm for 1 hour before inducing expression with 0.2 mM isopropyl β-D-1-thiogalactopyranoside. The cells were harvested after 20 hours expression, resuspended in buffer A (20 mM Tris pH 7.5, 100 mM NaCl), complete EDTA-free protease inhibitor cocktail (Roche), and DNase, lysed using an Avestin Emulsiflex C-5 at 15,000 psi, pelleted by ultracentrifugation, and homogenized. The fusion protein was extracted with 1% *n*-dodecyl-β-D-maltoside (DDM). Solubilized protein was purified using amylose resin and eluted using buffer A containing 40 mM maltose and 0.02% DDM. His-MBP-(ELIC-α_1 GABA$_A$ receptor) was digested overnight with tobacco etch virus protease, cleaned up using a reverse nickel on nitrilotriacetic acid (Ni-NTA) purification, and injected onto a Sephadex 200 Increase 10/300 column, which yielded pentameric protein in buffer A + 0.02% DDM.

Photolabeling and Intact Protein MS Analysis. The synthesis of neurosteroid photolabeling reagent (3α,5α,17β)-17-[[4-[3-(trifluoromethyl)-3*H*-diazirin-3-yl] phenyl] methoxy]-androstane-3-ol (KK200) has been detailed previously (Cheng et al., 2018). Purified ELIC-α1 GABA$_A$ receptor was photolabeled and analyzed by intact protein mass spectrometry (MS) as described previously (Budelier et al., 2017; Cheng et al., 2018; Sugasawa et al., 2019). Briefly, 50 μg of detergent-solubilized ELIC-α1 GABA$_A$ receptor (0.4 mg/ml in buffer A + DDM) was incubated with 100 μM KK200 in a glass tube for 60 minutes at 4°C in the dark. The sample was transferred to a quartz cuvette and then placed in a photoreactor at a distance of 7 cm from the source. The photoreactor uses a 450W Hanovia medium-pressure mercury lamp as the light source. A cold-water jacket cooled the lamp, and the light was filtered through a 1.5 cm thick saturated copper sulfate solution. This filter absorbs all light of wavelength < 315 nm (Katzenellenbogen et al., 1974). Illuminance at the middle of the cuvette was approximately 10 lumens/cm^2 as measured with a Newport model 1918-C optical meter. The samples were irradiated for 5 minutes and continuously cooled to 4°C. For the intact protein MS analysis, the irradiated samples were treated with 250 mM dithiothreitol (DTT) and then precipitated with chloroform/methanol/water. The precipitated protein was washed three times with equal volumes of water and methanol, centrifuged, and the protein pellet was reconstituted in 3 μl of 90% formic acid followed by 100 μl of 4:4:1 chloroform/methanol/water. Reconstituted samples were then analyzed in an Orbitrap Elite mass spectrometer (Thermo Fisher Scientific) by direct injection at 3 μl/min using a Max Ion atmospheric pressure ionization source with a heated electrospray ionization-II probe. Full spectra of photolabeled ELIC-α1 GABA$_A$ receptor were acquired on the linear trap quadrupole using spray voltage of 4 kV, capillary temperature of 320°C, and in-source dissociation of 30 V. Deconvolution of intact ELIC-α1 GABA$_A$ receptor spectra was performed using UniDec (Marty et al., 2015).

Tryptic Middle-Down MS Analysis. Photolabeled ELIC-α1 GABA$_A$ receptor was analyzed by middle-down MS as detailed in previous reports (Budelier et al., 2017; Cheng et al., 2018; Chen et al., 2019; Sugasawa et al., 2019, 2020). 20 μg (0.4 mg/ml) of photolabeled ELIC-α1 GABA$_A$ receptor was buffer-exchanged to 50 mM triethylammonium bicarbonate buffer with 0.02% DDM using Micro Bio-Spin 6 columns (Bio-Rad). The buffer-exchanged sample was reduced with 5 mM tris(2-carboxyethyl)phosphine for 1 hour, alkylated with 5 mM *N*-ethylmaleimide for 1 hour, and quenched with 5 mM DTT for 15 minutes. Samples were then digested with 8 μg of trypsin for 7 days at 4°C; extended digestion at low temperature was necessary to obtain maximal recovery of TMD peptides. Next, formic

acid was added to 1%, followed directly by liquid chromatography - mass spectrometry analysis on an Orbitrap Elite mass spectrometer. 20-μl samples were injected into a home-packed PLRP-S (Agilent) column (10 cm × 75 μm, 300 Å), separated with a 145-minute gradient from 10% to 90% acetonitrile, and introduced to the mass spectrometer at 800 nl/min with a nanospray source. MS acquisition was set as an MS1 Orbitrap scan (resolution of 60,000) followed by top 20 MS2 Orbitrap scans (resolution of 15,000) using data-dependent acquisition, and exclusion of singly charged precursors.

Fragmentation was performed using high-energy dissociation with normalized energy of 35%. Analysis of data sets was performed using Xcalibur (Thermo Fisher Scientific) to manually search for TM1, TM2, TM3, or TM4 tryptic peptides with or without neurosteroid photolabeling modifications. Photolabeling efficiency was estimated by generating extracted chromatograms of unlabeled and labeled peptides, determining the area under the curve, and calculating the abundance of labeled peptide/(unlabeled + labeled peptide). MS2 spectra of photolabeled TMD peptides were analyzed by manual assignment of fragment ions with and without photolabeling modification. Fragment ions were accepted based on the presence of a monoisotopic mass within 20 ppm mass accuracy. In addition to manual analysis, PEAKS (Bioinformatics Solutions Inc.) data base searches were performed for data sets of photolabeled ELIC-α1 $GABA_A$ receptor. Search parameters were set for a precursor mass accuracy of 20 ppm, fragment ion accuracy of 0.1 Da, up to 3 missed cleavages on either end of the peptide, false discovery rate of 0.1%, and variable modifications of methionine oxidation, cysteine alkylation with *N*-ethylmaleimide and DTT, and neurosteroid analog photolabeling reagent on any amino acid.

Simulations of Function and Muscimol Binding. Simulations of peak current responses were carried out using a modified state function in which the effects of agonist X were mediated by two classes of sites:

$$P_{A,peak} = \frac{1}{1 + L^{*}\left[\frac{1+[X]/K_{R,X,1}}{1+[X]/(c_{X,1}K_{R,X,1})}\right]^{N_1}\left[\frac{1+[X]/K_{R,X,2}}{1+[X]/(c_{X,2}K_{R,X,2})}\right]^{N_2}} \quad (2)$$

where $K_{R,X,1}$ and $K_{R,X,2}$ are the equilibrium dissociation constants of X for the two classes of binding sites in the resting receptor, and $c_{X,1}$ and $c_{X,2}$ are the measures of efficacy. N_1 and N_2 give the number of binding sites per receptor for X within each class of binding sites. L* was constrained to 1000 to mimic direct activation by X or to 19 to mimic X-induced potentiation of background activity with $P_{A,peak}$ of 0.05.

Muscimol binding in the presence of an allosteric agonist X was simulated as described previously (Akk et al., 2020):

$$Y_M = \frac{QL^{*}\alpha_M(1+\alpha_M)^{N_M-1} + Q(\frac{\alpha_M}{c_M})(1+(\frac{\alpha_M}{c_M}))^{N_M-1} + (\frac{\alpha_M}{d_M c_M})(1+(\frac{\alpha_M}{d_M c_M}))^{N_M-1}}{QL^{*}(1+\alpha_M)^{N_M} + Q(1+(\frac{\alpha_M}{c_M}))^{N_M} + (1+(\frac{\alpha_M}{d_M c_M}))^{N_M}} \quad (3)$$

where Y_M is the fraction of orthosteric binding sites occupied by muscimol, Q is the ratio of receptors in the active state relative to desensitized state when neither muscimol nor X is bound [assumed 0.29; (Germann et al., 2019)], α_X = [muscimol]/$K_{R,muscimol}$, N_M is the number of muscimol binding sites [assumed 2; (Chang et al., 1996)], c_M is the ratio of the equilibrium dissociation constant for muscimol in the active receptor ($K_{A,muscimol}$) to $K_{R,muscimol}$, and d_M is the ratio of the equilibrium dissociation constant for muscimol in the desensitized receptor to $K_{A,muscimol}$ [assumed to be 1; (Germann et al., 2019)]. In simulations, the muscimol concentration was selected to generate 10% equilibrium occupancy of muscimol binding sites in the absence of X.

L* for eq. 3 was calculated as:

$$L^{*} = L\left[\frac{1+[X]/K_{R,X,1}}{1+[X]/(c_{X,1}K_{R,X,1})}\right]^{N_1}\left[\frac{1+[X]/K_{R,X,2}}{1+[X]/(c_{X,2}K_{R,X,2})}\right]^{N_2} \quad (4)$$

where L is the ratio of resting to active receptors in the absence of agonist [assumed 8000; (Shin et al., 2017)]. Other terms are as described above. In essence, the presence of the allosteric agonist X enhances background activity by reducing the value of L, which then increases muscimol occupancy of high-affinity states (active and desensitized).

Docking Studies of 3α5αP. Site I (β-α interface) was modeled using the cryoEM structure of the human α1β3γ2 GABA receptor [PDB ID:6I53, (Laverty et al., 2019)]. The site is defined by TM1 of the α1 subunit and TM3 of the β2 subunit. In this region, there are only two sequence differences between the human β3 and rat β2, L294M and F301L. These mutations were made in the modeling program chimera to the structure. Homology models of the rat α1 and β2 subunits were built using a multitemplate approach using the Modeler program. The structures used as templates were the human α1β3γ2 GABA receptor [PDB ID:6I53; and 6HUO, (Masiulis et al., 2019)] and the human α1β1γ2 GABA receptor [PDB ID: 6DW0, (Phulera et al., 2018)]. The best scoring of 100 produced models of each subunit was then used for docking. The docking sites were defined by the photolabeled residues (Sugasawa et al., 2020). 3α5αP was then docked into each site with the program Autodock Vina using a box size of 15 × 15 × 15 Å, an energy range of 3 kcal, exhaustiveness of 25, and a num_mode of 20.

Drugs. The stock solution of GABA was made in ND96 at 500 mM and stored in aliquots at −20°C. The steroids 3α5αP and alfaxalone were dissolved in DMSO at 20 mM and 10 mM, respectively, and stored at room temperature. Final dilutions were made on the day of experiment.

Results

Activation of Wild-Type and Mutant Receptors by GABA. The following mutations to the three putative binding sites for potentiating steroids were tested: α1(Q241L) and α1(Q241S) in site I (β-α interface), α1(V226W) in site II (intra-α subunit site), and β2(M283A), β2(G287W), β2(Y443W), and β2(Y447A) in site III (intra-β subunit site). We commenced by verifying receptor expression and function by measuring activation of the mutant receptors by GABA. Cells expressing α1β2γ2L wild-type or mutant receptors were exposed to a range of concentrations of GABA, and the peak current amplitudes were determined and analyzed using the Hill equation. The EC_{50}s and Hill coefficients of the fits are given in Table 1.

TABLE 1
Activation of α1β2γ2L wild-type and mutant receptors by GABAThe table gives the EC_{50}s and Hill coefficients (mean ± S.D. from 5–8 cells per receptor) for wild-type and mutant receptors.

Receptor	GABA EC_{50}	n_{Hill}
	μ*M*	
α1β2γ2L wild-type	16.3 ± 7.4	1.32 ± 0.02
α1(Q241L)β2γ2L	444 ± 199	0.76 ± 0.02
α1(Q241S)β2γ2L	23.7 ± 11.9	1.37 ± 0.13
α1(V226W)β2γ2L	150 ± 72	0.80 ± 0.05
α1(Q241L+V226W)β2γ2L	309 ± 241	0.78 ± 0.06
α1(Q241S+V226W)β2γ2L	237 ± 129	0.82 ± 0.06
α1β2(M283A)γ2L	22.5 ± 12.2	1.13 ± 0.13
α1β2(G287W)γ2L	51.4 ± 17.2	1.25 ± 0.08
α1β2(Y443W)γ2L	77.1 ± 44.1	0.81 ± 0.15
α1β2(Y447A)γ2L	28.8 ± 18.0	1.24 ± 0.15

Overall, the mutations shifted the GABA concentration-response relationships to higher transmitter concentrations. The largest effects were seen in receptors containing the α1(Q241L) mutation. Mutations to site III in the β subunit had relatively minor effects on receptor activation by GABA. The observations are in agreement with previous studies where these mutations have been used (Hosie et al., 2006; Akk et al., 2008; Bracamontes et al., 2011; Chen et al., 2019).

Analysis of Receptor Activation by GABA + 3α5αP. Receptor potentiation by 3α5αP was tested by coapplying 0.01 – 10 μM 3α5αP with a low concentration of GABA and measuring steroid-induced enhancement of the peak response. The concentration of GABA was selected to generate a response that was 2%–10% of the peak response to 1 mM GABA + 50 μM propofol (P_A = 0.02 – 0.1). Sample current traces and the steroid concentration-response curves are given in Fig. 2. Table 2 gives the low- and high-concentration asymptotes ($P_{A,low}$ and $P_{A,high}$) and the steroid EC_{50}s in the wild-type and mutant receptors. The mutations had generally small effects on the steroid EC_{50}.

We used a resting-active cyclic model to quantitatively analyze the 3α5αP concentration-response relationships (Forman, 2012; Steinbach and Akk, 2019). The model is based on the classic Monod-Wyman-Changeux model, originally used to describe enzyme function and modulation (Monod et al., 1965). The analysis provides estimates of the affinity of the steroid to the resting receptor ($K_{R,3\alpha5\alpha P}$) and its gating efficacy ($c_{3\alpha5\alpha P}$).

The results are summarized in Table 2. The effects of mutations on calculated affinity of the resting receptor to 3α5αP were generally unremarkable. The α1(Q241L) and α1(V226W) mutations to sites I (the intersubunit binding site) and II (intra-α site), respectively, reduced 3α5αP gating efficacy. None of the tested mutations to site III affected efficacy of the steroid.

The reduced but still considerable (2.3 ± 0.6-fold at 1 μM; n = 6 cells; 1 = no effect) potentiating effect of 3α5αP in the α1(Q241L)β2γ2L receptor was surprising given that some previous studies had indicated that the mutation essentially abolishes modulation by classic potentiating steroids (Hosie et al., 2006; Akk et al., 2008; Bracamontes et al., 2011), but see (Bracamontes and Steinbach, 2009). To attempt to exclude any time-dependent effects associated with long recordings and/or errors rising from comparing responses to drug applications separated by several minute-long washes, we tested the effect of 3α5αP on GABA-elicited steady-state current in a continuous recording where no washout between GABA and GABA + steroid was employed. A sample recording showing the potentiating effect of 3α5αP in this experimental protocol is given in Fig. 3A. In six cells, 1 μM 3α5αP potentiated the steady-state current elicited by 50 μM GABA ($P_{A,peak}$ = 0.09 ± 0.04) by 1.4 ± 0.3-fold.

During the initial, long GABA application, the receptors equilibrate between resting, active, and desensitized states. The extent of observed potentiation in this experimental protocol is therefore not directly comparable to potentiation observed when peak currents are compared (Fig. 2). Even so, the findings support the notion that the α1(Q241L)β2γ2L receptor retains considerable sensitivity to the steroid 3α5αP.

For further confirmation of sensitivity to potentiating steroids, we tested the ability of the synthetic steroid alfaxalone to potentiate the α1(Q241L)β2γ2L receptor. In five cells, 3 μM alfaxalone potentiated the peak response to 20 μM GABA ($P_{A,peak}$ = 0.03 ± 0.01) by 2.1 ± 0.3-fold. A sample trace is given in Fig. 3B. For comparison, in the wild-type α1β2γ2L receptor, 3 μM alfaxalone potentiates the response to low GABA by 13-fold (Shin et al., 2017).

Energetic Contributions of the Steroid Binding Sites. The parameter expressing agonist efficacy (c) and the postulated number of binding sites (N) for the agonist under consideration are connected through the empirical maximal probability of being in the active state as:

$$P_{A,\,peak,\,max} = \frac{1}{1 + L^{*}(c_{effect}{}^{N_{effect}})} \tag{5}$$

where L* is determined from the baseline activity as described for eq. 1, and c_{effect} and N_{effect} are the effective values from the total number of sites available. In the present case, in which 3α5αP binds to distinct sites, this is:

$$c_{effect}{}^{N_{effect}} = c_I{}^{N_I} c_{II}{}^{N_{II}} c_{III}{}^{N_{III}} = (c_I c_{II} c_{III})^2. \tag{6}$$

Since there are two copies of each site in the receptor, the number of steroid binding sites was constrained to 2 and the product of the three values was estimated. $\Delta G_{A,binding}$ expresses the total free energy change to stabilize the active state when all steroid binding sites are occupied:

$$\Delta G_{A,\,binding} = -2RT\ln(c_I c_{II} c_{III}). \tag{7}$$

The values provided in Table 2 indicate that the binding of 3α5αP to the α1β2γ2L receptor provides a total free energy change of −1.9 kcal/mol to stabilize the active state. The energetic contribution is less, i.e., the ΔG is less negative in receptors containing a mutation to site I or site II.

Model-independent analysis provides similar information about ΔΔG, but without any insights into affinity of the interaction. The energetic difference between the active and the resting states of the receptor is proportional to the ratio of the frequencies of the states:

$$\Delta G_A = -RT\ln(P_A/P_R) = -RT\ln(P_A/(1 - P_A)), \tag{8}$$

where in a two-state system such as this, $P_R = (1 - P_A)$. At a saturating concentration of 3α5αP, the total free energy change can be obtained from $(P_{A,max}/(1 - P_{A,max})$. To obtain the free energy provided by binding to all the sites, the baseline free energy difference must be subtracted:

$$\Delta\Delta G_{A,\,binding} = (-RT\ln(P_{A,\,max}/(1 - P_{A,\,max}))) - (-RT\ln(P_{A,\,0}/(1 - P_{A,\,0}))) \tag{9}$$

where $P_{A,0}$ is the probability of being active in the absence of the steroid (but in the same baseline condition, for example the presence of a low concentration of GABA). As indicated by the values in Table 2, there is good agreement between the two estimates (R^2 = 0.97).

The effects of the mutations on $\Delta\Delta G_{A,binding}$ suggest that binding to site I contributes the greater portion of the stabilization energy provided by 3α5αP (about −1.3 kcal/mol out of −2.0 kcal/mol), whereas occupation of site II contributes about −0.5 kcal/mol, and occupation of site III does not make a meaningful contribution.

Additivity of the Functional Effects of Mutations to Individual Steroid Binding Sites. We employed double mutant cycle analysis to determine pairwise additivity of the

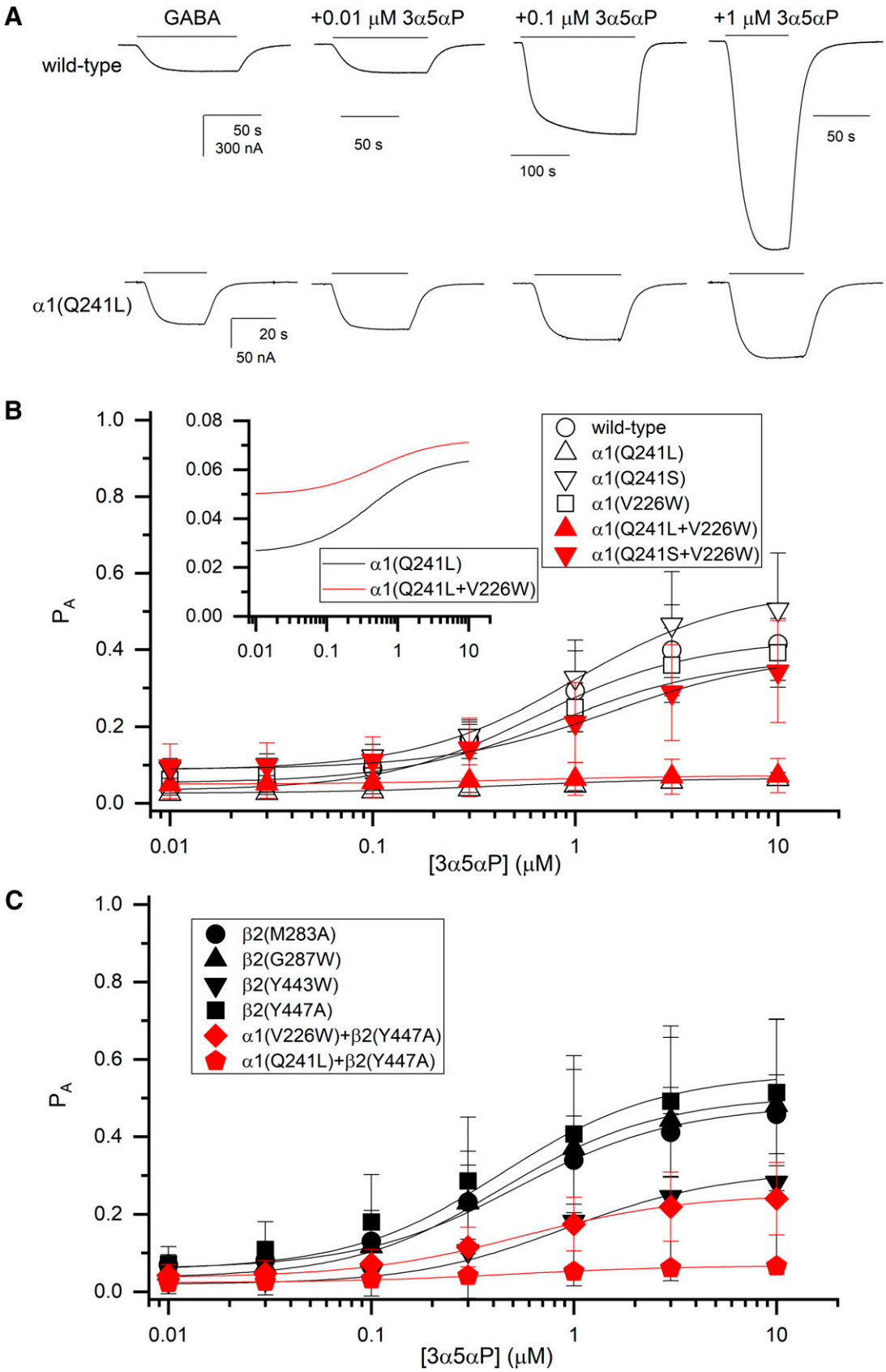

Fig. 2. Modulation of GABA-activated wild-type and mutant $\alpha1\beta2\gamma2$L receptors by 3α5αP. The panels show sample current traces (A) and steroid concentration-response curves for wild-type $\alpha1\beta2\gamma2$L and mutant receptors with mutations to steroid sites I and II (B) or site III (C). In (B) and (C), the data points show mean ± SD from 5–7 cells. The curves are calculated using the mean fitted parameters provided in Table 2. The inset in (B) gives the concentration-response curves for receptors containing the $\alpha1$(Q241L) and $\alpha1$(Q241L+V226W) mutations at higher resolution.

TABLE 2
Potentiation of α1β2γ2L wild-type and mutant receptors by 3α5αP
The table gives the low- and high-concentration asymptotes and EC_{50}s of the potentiation curves (mean ± S.D. from 5–7 cells per receptor) and the calculated ΔΔG from the ratios P_A/P_R using eq. 9. The data were also analyzed to provide estimated affinity of 3α5αP for the resting receptor ($K_{R,3\alpha5\alpha P}$) and the ratio of the affinities for the active and resting states ($c_{3\alpha5\alpha P}$) by fitting the concentration-response curves to eq. 1. The values of ΔG were calculated from the values of $c_{3\alpha5\alpha P}$ as $N_{3\alpha5\alpha P}RT\ln(c_{3\alpha5\alpha P})$. The number of 3α5αP sites was constrained to 2. Statistical significance of changes in $c_{3\alpha5\alpha P}$ was determined using ANOVA with Dunnett's correction (*$P < 0.05$; ***$P < 0.001$).

Receptor	Sites Mutated	$P_{A,low}$	EC_{50}	$P_{A,high}$	ΔΔG	$K_{R,3\alpha5\alpha P}$	$c_{3\alpha5\alpha P}$	ΔG
			μM		*kcal/mol*	μM		*kcal/mol*
α1β2γ2L wild-type	None	0.03 ± 0.02	0.72 ± 0.41	0.45 ± 0.08	−2.01 ± 0.29	0.58 ± 0.20	0.21 ± 0.05	−1.85 ± 0.26
α1(Q241L)β2γ2L	β-α	0.02 ± 0.004	0.58 ± 0.38	0.07 ± 0.02	−0.69 ± 0.16	0.35 ± 0.13	0.62 ± 0.06***	−0.57 ± 0.12
α1(Q241S)β2γ2L	β-α	0.10 ± 0.03	0.89 ± 0.15	0.52 ± 0.15	−1.42 ± 0.26	1.16 ± 0.40	0.27 ± 0.07	−1.57 ± 0.32
α1(V226W)β2γ2L	intra-α	0.06 ± 0.02	0.91 ± 0.32	0.41 ± 0.07	−1.46 ± 0.15	0.72 ± 0.21	0.33 ± 0.03*	−1.32 ± 0.12
α1(Q241L+V226W)β2γ2L	β-α, intra-α	0.05 ± 0.04	0.68 ± 0.45	0.08 ± 0.05	−0.32 ± 0.09	0.60 ± 0.40	0.76 ± 0.11***	−0.33 ± 0.18
α1(Q241S+V226W)β2γ2L	β-α, intra-α	0.08 ± 0.06	1.56 ± 0.82	0.34 ± 0.16	−1.15 ± 0.12	1.45 ± 0.43	0.39 ± 0.04*	−1.12 ± 0.12
α1β2(M283A)γ2L	intra-β	0.06 ± 0.03	0.46 ± 0.25	0.43 ± 0.13	−1.48 ± 0.16	0.53 ± 0.31	0.25 ± 0.03	−1.62 ± 0.14
α1β2(G287W)γ2L	intra-β	0.04 ± 0.04	0.45 ± 0.13	0.46 ± 0.18	−2.02 ± 0.26	0.44 ± 0.14	0.18 ± 0.02	−2.04 ± 0.11
α1β2(Y443W)γ2L	intra-β	0.02 ± 0.03	0.89 ± 0.32	0.29 ± 0.25	−1.98 ± 0.39	0.71 ± 0.26	0.20 ± 0.02	−1.90 ± 0.14
α1β2(Y447A)γ2L	intra-β	0.06 ± 0.04	0.53 ± 0.46	0.54 ± 0.19	−1.86 ± 0.28	0.50 ± 0.36	0.21 ± 0.07	−1.89 ± 0.43
α1(Q241L)β2(Y447A)γ2L	β-α, intra-β	0.02 ± 0.01	0.49 ± 0.14	0.07 ± 0.01	−0.80 ± 0.29	0.39 ± 0.11	0.57 ± 0.10***	−0.68 ± 0.23
α1(V226W)β2(Y447A)γ2L	intra-α, intra-β	0.04 ± 0.03	0.65 ± 0.28	0.24 ± 0.07	−1.20 ± 0.24	0.44 ± 0.15	0.33 ± 0.06*	−1.32 ± 0.19

Fig. 3. Potentiation of the α1(Q241L)β2γ2L receptor by 3α5αP and alfaxalone. (A) shows the effect of 1 μM 3α5αP on steady-state current elicited by 50 μM GABA. The peak P_A of the response to GABA was 0.063. (B) shows the effect of 3 μM alfaxalone (ALF) on peak responses to 20 μM GABA. The mean peak P_A of the responses to GABA before exposure to the steroid was 0.037.

effects of mutations to the individual steroid binding sites. In this approach, the free energy change in the double mutant is compared with the sum of changes in free energy in receptors containing a single mutation (Hidalgo and MacKinnon, 1995; Horovitz, 1996; Akk, 2001). A large difference in free energy change (typically > 0.5 kcal/mol) is interpreted as the mutated sites being directly or indirectly coupled (LiCata and Ackers, 1995; Schreiber and Fersht, 1995; Horovitz, 1996; Gleitsman et al., 2009).

Figure 4 shows pairwise mutant cycles for sites I and II, I and III, and II and III. For each mutant pair, we calculated the coupling energy, ΔΔG, as ΔG(wild-type) + ΔG(double mutant) − ΔG (mutant #1) − ΔG(mutant #2) using the values given in Table 2. The calculated ΔΔGs with 95% confidence intervals were 0.29 [−0.004 to 0.58] kcal/mol for α1(Q241L + V226W), 0.09 [−0.28 to 0.46] kcal/mol for α1(Q241S + V226W), 0.07 [−0.41 to 0.55] kcal/mol for α1(Q241L) + β2(Y447A), and −0.04 [−0.51 to 0.43] kcal/mol for α1(V226W) + β2(Y447A). Inclusion of 0 value in the confidence interval was interpreted to indicate a lack of significant coupling energy, i.e., additivity of the effects of mutations. We caution, however, that the relatively wide 95% confidence intervals, at least in part because of experimental imprecision, make it harder to demonstrate small deviation from additivity.

To estimate sensitivity of our approach, we determined the difference in ΔG between a hypothetical double mutant and sum of two single mutations that would result in no overlap between their 95% confidence intervals. The mean S.E.M. of ΔG in all tested receptors was 0.09, and the propagated S.E.M. for combined two mutations is 0.13. The 95% confidence interval can then be calculated for the double mutant as mean ± 1.96 × 0.09 and that for the sum of two single mutants as mean ± 1.96 × 0.13. This calculation gives 0.43 kcal/mol as the minimal ΔΔG between the sum of effects in

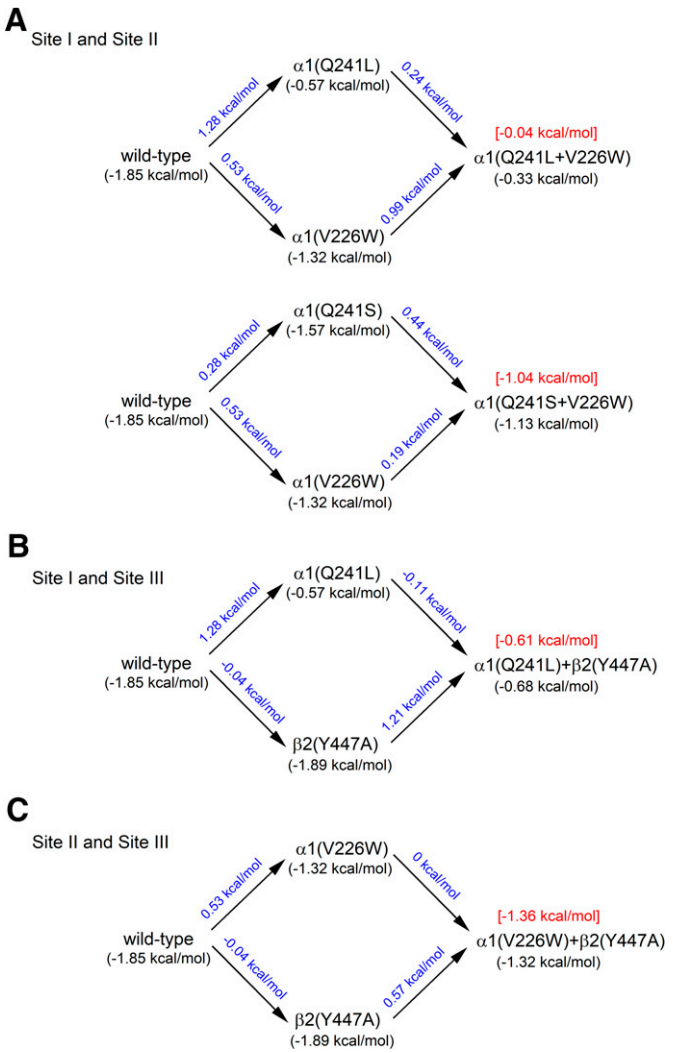

Fig. 4. Double mutant cycle analysis. Comparison of energetic effects of mutations introduced alone or in combination to sites I and II (A), sites I and III (B), and sites II and III (C). The ΔG in parentheses indicate the stabilization energy provided by 3α5αP in each receptor. ΔΔG values showing the effects of mutations are given in blue. The ΔG in brackets (red) for the double mutants gives the expected stabilization energy, calculated based on ideal additivity of the effects of single mutations. The closeness of the measured and calculated ΔG values for the double mutants indicates that the mutations act independently and additively.

two single mutants and the effect in double mutant, for us to observe a statistically significant ($P < 0.05$) effect.

Mutations to Sites I and II Do Not Cause Reciprocal Changes in Photolabeling. Amino acid substitutions leading to changes in local protein structure have been shown to modify the orientation in which a steroid binds in its binding site, which is the likely direct cause of reduced function (Sugasawa et al., 2019). Here, we considered whether mutations in sites I and II differently modify steroid binding in the proximal versus distal site. We reasoned that an independent effect of a mutation in site I may be expected to modify photolabeling in site I but not in site II, and vice versa. Indeed, it has been shown that in the ELIC-α1 chimeric homomeric receptor, the Q242L or Q242W mutations (homologous to Q241L and Q241W in the rat α1 subunit) in site I reorient the steroid analog and change the photolabeled residue from Y309 to F298 in site I, but do not modify the labeled residue (N408 in the fourth membrane-spanning domain) or its photolabeling efficiency (1.7%–1.9%) in site II (Sugasawa et al., 2019). Since a saturating concentration of KK200 (100 μM) was used, the efficiency of labeling does not necessarily depend on the equilibrium occupancy (that is, the affinity of the photolabel).

To confirm the reciprocal relationship, i.e., that amino acid substitution in site II does not affect photolabeling in site I, we compared photolabeling of wild-type and V227W mutant (homologous to V226W in rat α1) ELIC-α1 receptors with the steroid analog KK200. In the wild-type receptor, KK200 labeled N408 in site II and Y309 in site I. In the V227W mutant, KK200 labeling in site II was shifted to F400 at ∼2 α-helical turns toward the cytosol (Supplemental Fig. 1), and the labeling efficiency in site II was significantly increased. Neither the residue labeled in site I (Y309) nor the labeling efficiency were affected (Table 3).

Relating Energetic Additivity to Changes in Concentration-Response Measurements. Energetic additivity of mutations can be demonstrated by approaches such as mutant cycle analysis. However, we sought to gain insight into how energetic additivity manifests directly in some commonly measured activation parameters, for example, simple additive or multiplicative relationships among maximal open probabilities for single or multiple mutations. To do this, we simulated direct activation and potentiation concentration-response curves for cases mimicking selective modification of one or more binding sites.

In the first case, we modeled activation of a receptor with two binding sites for agonist X. Both binding sites had a $K_{R,X}$ (equilibrium dissociation constant for X in the resting receptor) of 10 units, and a c (ratio of the equilibrium dissociation constant for X in the active receptor to $K_{R,X}$) of 0.01. The value of L was held at 1000 (background P_A ∼0.001). From the relationship $P_{A,peak,max} = 1/(1 + Lc^N) = 1/(1 + Lc_1c_2)$, we calculate that the maximal peak open probability in this receptor (designated wild-type) is 0.91. We next postulated that introduction of a loss-of-function mutation to a single binding site increases the value of c of that site to 0.9. With either c_1 or c_2 thus modified, the $P_{A,peak,max}$ in the receptor containing a mutation to one of the binding sites in presence of saturating X is 0.10 (a reduction of ∼9-fold). Lastly, we combined mutations to both sites, i.e., $c_1 = c_2 = 0.9$. The $P_{A,peak,max}$ is 0.0012 (a reduction of ∼740-fold). Thus, the observed effect in the double mutant is much larger, in that the effects are neither additive or multiplicative, than what might be intuitively expected by independent actions of the single mutations. The simulated concentration-response curves are shown in Fig. 5A.

The extent of mismatch depends on the starting values of c. For an agonist-receptor pair with $c_1 = c_2 = 0.1$, the $P_{A,peak,max}$ is 0.091. With a single mutation increasing c to 0.9 in that site, the $P_{A,peak,max}$ is reduced to 0.011 (an ∼8-fold reduction), and with both sites mutated ($c_1 = c_2 = 0.9$) $P_{A,peak,max}$ is 0.0012 (an ∼74-fold reduction). The predictions are illustrated in Fig. 5B.

The dependence on the value of c is illustrated in Fig. 5C, which plots the fold-reduction in the value of $P_{A,peak,max}$ as a function of the initial value for c for both sites. As can be seen, the effect of the double mutation approaches the effect

TABLE 3
Photolabeling efficiency
The table provides photolabeling efficiency in % (total incorporation) of 100 μM KK200 in intact protein and middle-down MS analyses for ELIC-α1 GABA$_A$ receptor (n = 2, biologic replicates). The labeling efficiency in TM3 corresponds to labeling at site I and the labeling efficiency in TM4 corresponds to labeling at site II. Photolabeled residues are shown in parentheses. The data for wild-type and Q242L were reported previously (Sugasawa et al., 2019). The Q242 position in ELIC-α1 is homologous to Q241, and V227 is homologous to V226 in the rat α1 subunit.

		Middle-Down MS	
ELIC-α1 GABA$_A$R	Intact Protein MS	TM3 - Site I	TM4 - Site II
Wild-type	11.3, 10.7	8.0, 7.6 (Y309)	1.8, 1.6 (N408)
Q242L	11.8, 10.2	6.1, 5.5 (F298)	1.9, 1.5 (N408)
V227W	19.9, 15.4	8.5, 5.3 (Y309)	6.7, 4.2 (F400)

squared of a single mutation as the initial value of c approaches 1 (that is, as agonist X becomes a weaker agonist).

In the second case, we postulated a reduced value of L (L = 19) that generates a background P_A of 0.05, and examined the effect of X (Fig. 5, D–F). This situation models the potentiation by X of a response to a background agonist that produces a response of 5% of maximal receptor activation. Alternatively, background activity may be elicited by a gain-of-function mutation for which the direct-activating effect of X is measured. The binding of X to two sites, each with $K_{R,X}$ of 10 units and c_X of 0.01, increased the P_A to 0.9981 (~20-fold potentiation of background activity). Introduction of a loss-of-function mutation to one binding site, increasing c of that site to 0.9, reduced P_A to 0.854 (~17-fold potentiation of background activity; ~1.2-fold reduction from wild-type). When both sites for X are mutated (c_1 = c_2 = 0.9), the predicted P_A is 0.06 (~1.2-fold potentiation; ~15-fold reduction). So, in this model, mutation of one of two independent sites with identical properties has a relatively small effect, whereas modification of both sites virtually eliminates the ability of X to potentiate the receptor.

Again, the apparent mismatch depends on the beginning values of c. With c_1 = c_2 = 0.1, the application of X increases the P_A of the response to 0.84 (17-fold potentiation). With c_1 = 0.1 and c_2 = 0.9, X increases the P_A to 0.37 (7.4-fold potentiation), and with c_1 = c_2 = 0.9, to 0.06 (1.2-fold potentiation).

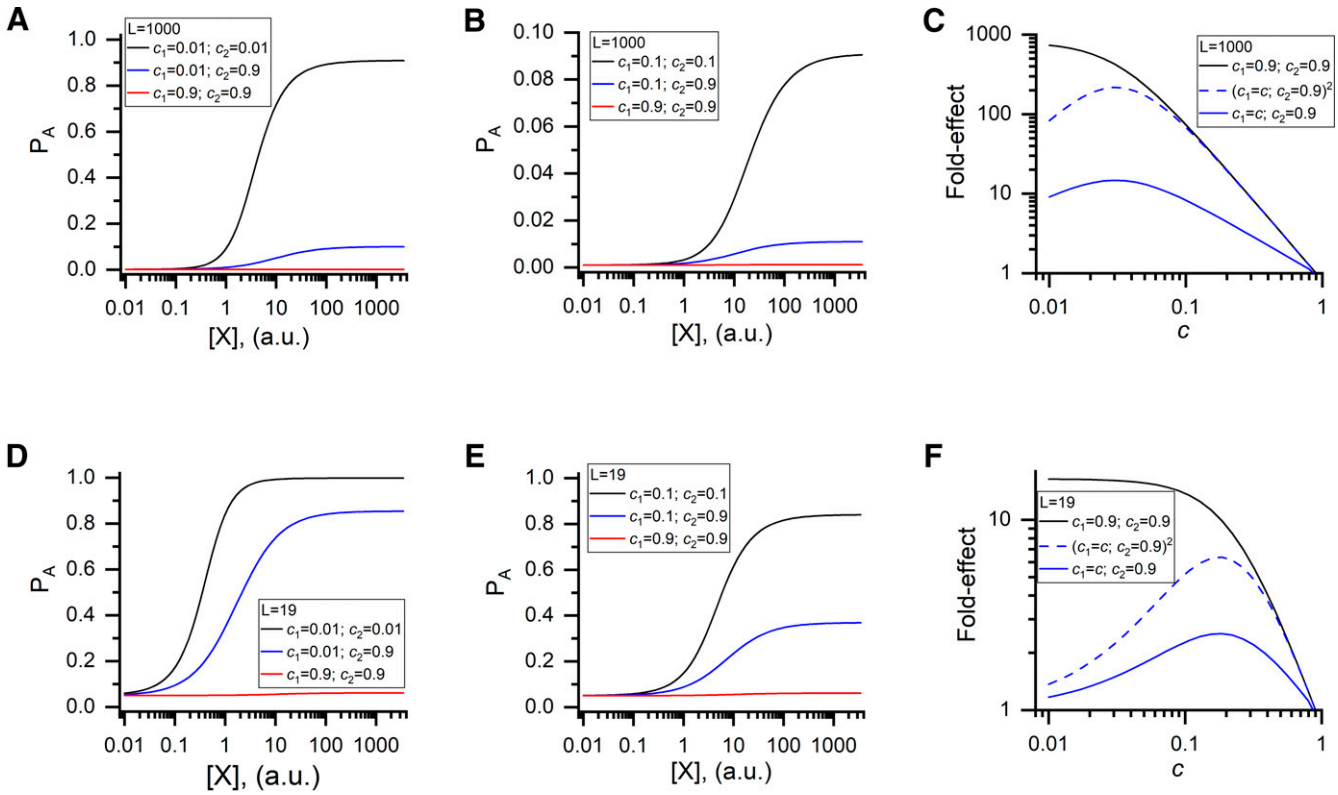

Fig. 5. Summary of effects of modifications to one or both binding sites on receptor activation. The graphs show modeled peak open probability (P_A) versus agonist (X) concentration. Modeling was done using $K_{R,X}$ of 10 arbitrary units (a.u.) and N_X of 2. The graphs compare the effects of loss-of-function modifications to one or both agonist binding sites. (A–C) describe a model with L of 1000 mimicking direct activation by X, and (D–F) describe a model with L of 19 mimicking X-mediated potentiation of receptor activity elicited by another agonist. (A, B, D, and E) show the effects of changing the value of c in one (blue lines) or both binding sites (red line) from 0.01 to 0.9. The precise maximal P_A values for each condition are given in text. (C and F) describe the reduction in maximal P_A (fold-effect) in receptors containing one (blue solid line) or both (black line) modified binding sites. The value of modified c was held at 0.9. The value of unmodified, i.e., wild-type c is given by the abscissa. The blue dashed line gives a squared fold-effect observed when one binding site is modified.

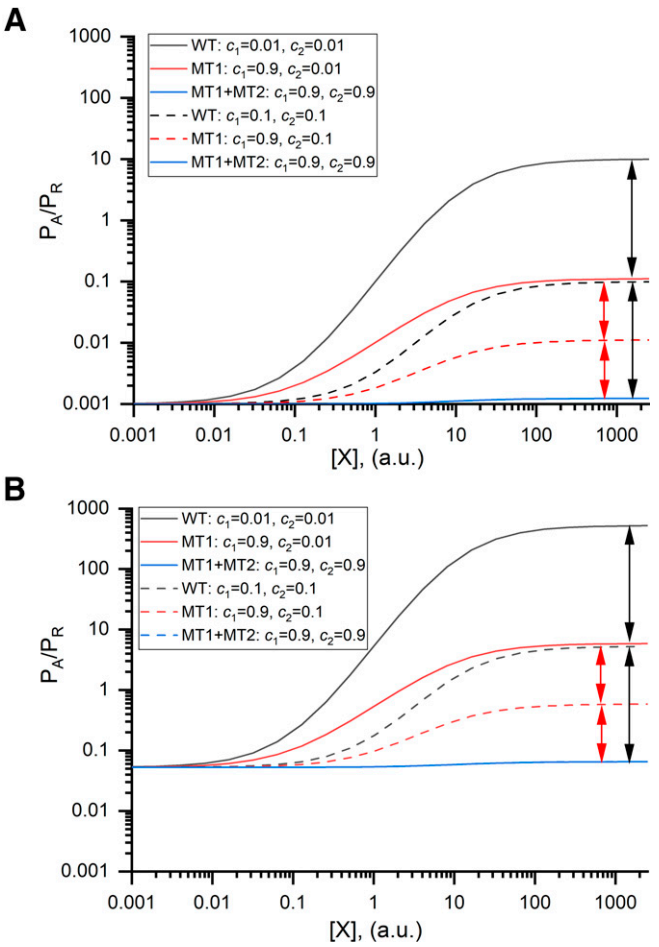

Fig. 6. Summary of effects of modifications to one or both binding sites on receptor P_A/P_R. The graphs show calculated values of P_A/P_R for the same conditions as were used in Figure 5. (A) shows a logarithmic plot for values when L = 1000, with values for c_1 and c_2 indicated. The low concentration asymptote is 1/L (0.001) for all the curves, whereas the high-concentration asymptote is $1/(Lc_1c_2)$. The arrows show the multiplicative relationship between the maximal values (90-fold when the nonmutated c = 0.01 and 9-fold when the nonmutated c = 0.1). (B) shows similar calculations for L=19. Note that the curves in (B) are shifted upwards by the ratio 1000/19 but are otherwise identical. MT, mutant; WT, wild-type.

Comparison of the curves in Fig. 5C and 5F indicates that the extent of the discrepancy depends on both the receptor baseline opening equilibrium and the affinity ratio for the unmutated receptor.F

An alternative experimental parameter is the ratio P_A/P_R as introduced earlier. Figure 6 shows simulations of this ratio for the same conditions used in the case of $P_{A,peak,max}$. Note that the curves for the two values of L are shifted vertically by the multiplicative factor (1/L). The relative maximal values for no, one, and two mutations is $[1/(c_{wt}c_{mut})]$, that is 90-fold when c_{WT} = 0.01 or 9-fold when c_{WT} = 0.1. Accordingly, for this experimental parameter, energetic additivity results in multiplicative changes in effect that are clearly seen in logarithmic plots.

Relating Energetic Additivity to Changes in the Binding of Orthosteric Agonist. Changes in equilibrium binding of a radiolabeled orthosteric agonist of the $GABA_A$ receptor, such as [^{3}H]muscimol, in the presence of allosteric modulators have provided insight into the mechanisms and sites of action of allosteric drugs (Harrison and Simmonds, 1984; Peters et al., 1988; Sugasawa et al., 2020). Here, we modeled the effect of allosteric agonist X on binding of muscimol, using a three-state resting-active-desensitized model (Akk et al., 2020). The concentration of muscimol was selected to generate equilibrium occupancy of 10% in the absence of X. We postulated two classes of binding sites for X, with one copy of each in the receptor. The effect of a loss-of-function mutation introduced to one or both binding sites for X was then simulated by changing the value of c of one or both sites from 0.01 to 0.9.

The results of simulations are shown in Fig. 7. Exposure to allosteric agonist X is predicted to enhance muscimol binding because it increases the prevalence of the high-affinity active and desensitized states, and so increases receptor occupancy in the presence of a fixed concentration of orthosteric agonist. The maximal potentiating effect in the receptor with c of both binding sites of 0.01 (a wild-type receptor) is 8.7-fold. In

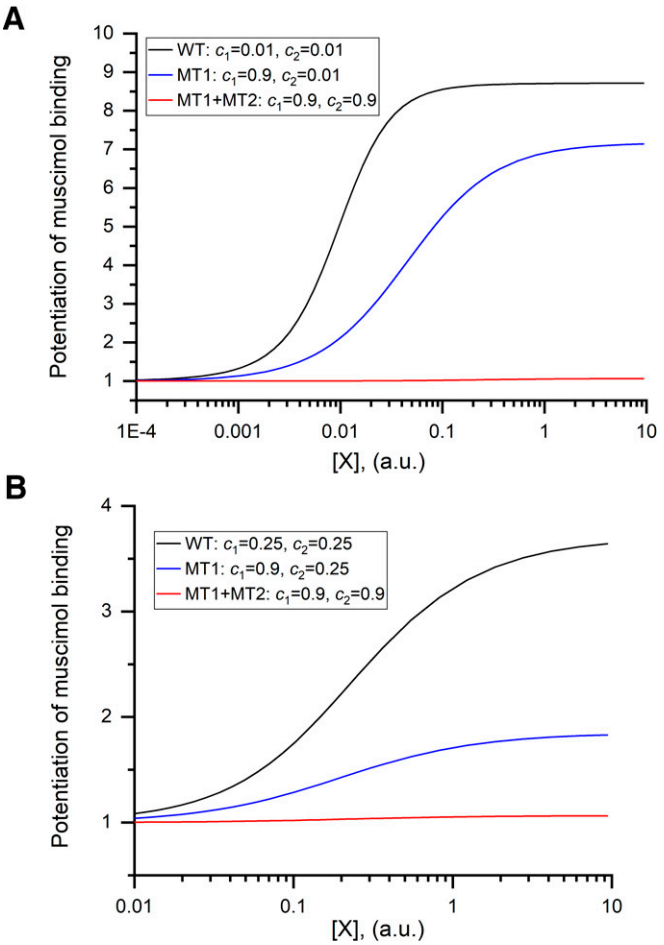

Fig. 7. Summary of effects of modifications to one or both binding sites for allosteric agonist on binding of orthosteric agonist. The simulations show potentiation of muscimol binding by allosteric agonist X. The simulations were based on $\alpha1\beta2\gamma2$L $GABA_A$ receptor with L = 8000 and Q = 0.29 (Shin et al., 2017; Germann et al., 2019). The properties ($K_{R,muscimol}$ = 0.5 μM, $c_{muscimol}$ = 0.01, $N_{muscimol}$ = 2 binding sites) and concentration (0.039 μM) of muscimol were selected so as to generate equilibrium occupancy of 10% of binding sites. The allosteric agonist X was assigned $K_{R,X}$ = 0.5 units and N_X = 2 binding sites, with c_1 = c_2 = 0.01 (A) or c_1 = c_2 = 0.25 (B). Introduction of a loss-of-function mutation to one or both binding sites was simulated by changing the value of c in that binding site to 0.9.

the receptor with one site for X mutated ($c_1 = 0.9$, $c_2 = 0.01$), X enhances muscimol binding by 7.2-fold, and with both sites mutated, ($c_1 = c_2 = 0.9$) by 1.1-fold (Fig. 7A). Thus, introduction of a single mutation leads to a smaller effect than what might be reasonably expected assuming additive effects. The apparent discrepancy depends on the value of c. With c_X of 0.25 (i.e., mimicking weaker efficacy of X), muscimol binding is enhanced by 3.7-fold in the wild-type receptor and by 1.8-fold in the receptor containing one mutated site for X (Fig. 7B).

Discussion

We had two goals in this study. The first was to determine whether the previously identified binding sites for potentiating steroids act independently. An alternative hypothesis of allosteric interaction between sites I (β-α interface) and II (intra-α) was proposed by Chen et al., 2019, who had observed that mutations to either site reduced potentiation by 3α5αP more than what appeared intuitively additive. Here, we conclude that the binding sites for potentiating steroids contribute independently and additively to channel activation. Using a more extensive set of mutated residues, we confirm a previous finding (Chen et al., 2019) that the intra-β subunit binding site does not contribute to receptor potentiation by 3α5αP. Our second goal was to test whether energetic additivity between independent binding sites predicts qualitatively interpretable changes in concentration-response curves. From simulations made using the Monod-Wyman-Changeux activation model, we show that additive energetic changes at independently acting binding sites can lead to nonlinear summation of the effects. Many commonly used experimental values, such as the probability of being open or the EC_{50} for an effect, do not depend in a simple fashion on the energetics of steroid-receptor interaction. Further, the kinetic parameters depend exponentially on the free energies involved. This makes it difficult to intuitively deduce additivity when the plotted experimental values depend nonlinearly on free energy change.

We used a mutational approach to determine independence of effects (Horovitz, 1996). The three previously identified binding sites for potentiating steroids were mutated individually or in combination, and the effects of mutations on channel gating by 3α5αP quantified. We reasoned that energetic additivity of the effects of mutations in individual binding sites is an indication of independently acting sites, whereas, in the case of a specific allosteric link between sites, a mutation that alters the structure of site I and/or its interaction with the steroid may be expected to modify steroid interaction with site II. The electrophysiological data indicate that the effects of mutations to sites I (β-α interface), II (intra-α), and III (intra-β) are energetically additive.

Both additivity and nonadditivity between allosteric binding sites in the GABA$_A$ receptor have been reported previously. By individually mutating the two etomidate binding sites in the β-α interface in the concatemeric $\alpha1\beta2\gamma2$ receptor, Guitchounts et al., 2012 reported indistinguishable and additive effects of the α1(M236W) mutation on potentiation by etomidate. Similarly, the β2(Y143W) and β2(M286W) mutations to the two individual β subunits were shown to weaken receptor activation by propofol approximately equally and additively (Shin et al., 2018). In contrast, Szabo et al., 2019 showed nonadditive effects of TM2-15' and TM3-36' mutations at the α-β, β-α, and γ-β interfaces on anesthetic modulation of GABA currents. We do not have an explanation for this difference in observations.

The independent, additive effects of 3α5αP binding to sites I and II are supported by photolabeling data, which indicate that mutations to sites I and II modify photolabeling in the proximal site but not in the distal site. We previously showed that the α1(Q242L) mutation in the ELIC-α1 chimeric receptor modifies the residue photolabeled by a neurosteroid analog in site I, but has no effect on either photolabeling efficiency or the labeled residue in site II (Sugasawa et al., 2019). We now show that the V227W mutation in site II changes the photolabeled residue in site II, but does not affect the photolabeling efficiency or location of the labeled residue in site I. The V227W mutation increases the efficiency of photolabeling in site II (Table 3). Although this increased labeling efficiency could result from either an increase in ligand affinity for mutated site II or an increase in the photochemical efficiency of labeling, it is inconsistent with decreased steroid occupancy of the mutated site. Collectively, the photolabeling data indicate that mutations in site I and II produce their effects by changing ligand orientation in the site, thereby reducing steroid efficacy rather than by decreasing steroid occupancy. This is consistent with electrophysiological data showing that mutations in site I and II substantially reduce 3α5αP efficacy while producing only minor changes in steroid potency (Table 2).

Steroid-mediated potentiation was observed in the α1(Q241L)β2γ2L receptor. Some previous work, including our own, has reported complete elimination of potentiation of GABA-elicited currents by potentiating steroids after this mutation (Hosie et al., 2006; Akk et al., 2008; Bracamontes et al., 2011). Other prior work has shown small but measurable and statistically significant potentiation (Bracamontes and Steinbach, 2009). The ability of a steroid to potentiate the $\alpha1(Q241L)\beta2\gamma2$L receptor is critical to the conclusions of the present study, as it would not be feasible to measure the additivity of effects of mutations if modification of one site fully eliminated the response. Potentiation was observed in two experimental protocols, including one in which the effect of the steroid was measured on steady-state response to low GABA, i.e., without a preceding wash (Fig. 3). Qualitatively, this experiment most strongly demonstrates that the α1(Q241L)-containing receptor retains sensitivity to 3α5αP.

To gain insight into relative contributions made by sites I and II to channel potentiation by 3α5αP, we compared the effects of mutations made to each site. In the wild-type receptor, 3α5αP provides -1.9 to -2.0 kcal/mol of free energy change. In $\alpha1(Q241L)\beta2\gamma2$L, 3$\alpha$5$\alpha$P provides -0.6 to -0.7 kcal/mol. Therefore, if the α1(Q241L) mutation fully disables steroid actions through site I, steroid action at site II contributes only -0.7 kcal/mol. This value is comparable to the loss of contribution made by the steroid in the receptor with the α1(V226W) mutation [$\Delta\Delta G_{\text{Site II}} = \Delta G_{\text{wild-type}} - \Delta G_{\alpha1(V226W)} = -0.5$ to -0.6 kcal/mol]. If we assume that the α1(V226W) mutation fully abolishes steroid effect through site II, then the remainder (-1.5 kcal/mol) can be assigned to energetic contributions through site I. This value is close to the loss of free energy change observed after the introduction of the α1(Q241L) mutation (-1.3 kcal/mol). Thus, we propose that

site I contributes more than 2-fold more free energy change than site II. We note that this estimate applies to the steroid 3α5αP; other ligands to sites I and II may differ in their energetic contributions.

One goal of this study was to gain insight into how energetic additivity of combined mutations manifests in commonly measured parameters, including magnitude of effect. In other words, if mutation #1 reduces function (activation or potentiation) by a-fold, mutation #2 by b-fold, and the combination of the two mutations by c-fold, what relationship between a, b, and c indicates independence and additivity versus allosteric interaction. Intuitively, we may expect that $a \times b = c$. For example, if mutation #1 reduces channel open probability by 3-fold, and mutation #2 reduces channel open probability by 2-fold, then it may be intuitively expected that the current is reduced by 6-fold in the double mutant if the mutations act independently.

Modeling of current responses using the MWC-based two-state model indicated that energetic additivity predicts responses for combinations of mutations that can be markedly different from the product of effect sizes of individual mutations. The results of simulations are presented in Fig. 5, C and F, where the distance between the blue dashed and black lines indicates the apparent mismatch between the effect predicted by the combination of mutations and the effect predicted by doubling the effect of a single mutation. The lines indicate that the mismatch is most prominent at low values of *c*, i.e., when the agonist being studied has high efficacy. In contrast, the experimental value P_A/P_R results in graphic display of data that qualitatively demonstrates energetic additivity (Fig. 6). The same logic applies to actions of allosteric agonists on enhancement of [^{3}H]muscimol binding. 3α5αP enhances the binding of the orthosteric agonist muscimol to the $GABA_A$ receptor by increasing the occupancy of high-affinity active and desensitized states (Akk et al., 2020). Mutations that reduce the ability of the steroid to bind or gate the receptor reduce the effect on muscimol binding (Sugasawa et al., 2020), whereas our simulations (Fig. 7) indicate that the sum of effects of independent mutations does not need to be algebraically additive.

Acknowledgments

We thank Amnon Horovitz (Weizmann Institute of Science) for advice on double mutant cycle analysis.

Authorship Contributions

Participated in research design: Evers, Steinbach, Akk.

Conducted experiments: Germann, Pierce, Tateiwa, Sugasawa.

Contributed new reagents or analytical tools: Reichert.

Performed data analysis: Germann, Pierce, Tateiwa, Sugasawa, Evers, Steinbach, Akk.

Wrote or contributed to the writing of the manuscript: Germann, Pierce, Tateiwa, Sugasawa, Reichert, Evers, Steinbach, Akk.

References

Akk G (2001) Aromatics at the murine nicotinic receptor agonist binding site: mutational analysis of the alphaY93 and alphaW149 residues. *J Physiol* **535**:729–740.

Akk G, Germann AL, Sugasawa Y, Pierce SR, Evers AS, and Steinbach JH (2020) Enhancement of muscimol binding and gating by allosteric modulators of the $GABA_A$ receptor: relating occupancy to state functions. *Mol Pharmacol* **98**:303–313.

Akk G, Li P, Bracamontes J, Reichert DE, Covey DF, and Steinbach JH (2008) Mutations of the $GABA_A$ receptor α1 subunit M1 domain reveal unexpected complexity for modulation by neuroactive steroids. *Mol Pharmacol* **74**:614–627.

Akk G, Shu HJ, Wang C, Steinbach JH, Zorumski CF, Covey DF, and Mennerick S (2005) Neurosteroid access to the $GABA_A$ receptor. *J Neurosci* **25**:11605–11613.

Bracamontes J, McCollum M, Esch C, Li P, Ann J, Steinbach JH, and Akk G (2011) Occupation of either site for the neurosteroid allopregnanolone potentiates the opening of the $GABA_A$ receptor induced from either transmitter binding site. *Mol Pharmacol* **80**:79–86.

Bracamontes JR and Steinbach JH (2009) Steroid interaction with a single potentiating site is sufficient to modulate $GABA_A$ receptor function. *Mol Pharmacol* **75**:973–981.

Budelier MM, Cheng WWL, Bergdoll L, Chen ZW, Janetka JW, Abramson J, Krishnan K, Mydock-McGrane L, Covey DF, Whitelegge JP, et al. (2017) Photoaffinity labeling with cholesterol analogues precisely maps a cholesterol-binding site in voltage-dependent anion channel-1. *J Biol Chem* **292**:9294–9304.

Chang Y, Wang R, Barot S, and Weiss DS (1996) Stoichiometry of a recombinant $GABA_A$ receptor. *J Neurosci* **16**:5415–5424.

Chen Q, Wells MM, Arjunan P, Tillman TS, Cohen AE, Xu Y, and Tang P (2018) Structural basis of neurosteroid anesthetic action on $GABA_A$ receptors. *Nat Commun* **9**:3972.

Chen ZW, Bracamontes JR, Budelier MM, Germann AL, Shin DJ, Kathiresan K, Qian MX, Manion B, Cheng WWL, Reichert DE, et al. (2019) Multiple functional neurosteroid binding sites on $GABA_A$ receptors. *PLoS Biol* **17**:e3000157.

Cheng WWL, Chen ZW, Bracamontes JR, Budelier MM, Krishnan K, Shin DJ, Wang C, Jiang X, Covey DF, Akk G, et al. (2018) Mapping two neurosteroid-modulatory sites in the prototypic pentameric ligand-gated ion channel GLIC. *J Biol Chem* **293**:3013–3027.

Forman SA (2012) Monod-Wyman-Changeux allosteric mechanisms of action and the pharmacology of etomidate. *Curr Opin Anaesthesiol* **25**:411–418.

Germann AL, Pierce SR, Senneff TC, Burbridge AB, Steinbach JH, and Akk G (2019) Steady-state activation and modulation of the synaptic-type α1β2γ2L $GABA_A$ receptor by combinations of physiological and clinical ligands. *Physiol Rep* **7**:e14230.

Gleitsman KR, Shanata JA, Frazier SJ, Lester HA, and Dougherty DA (2009) Long-range coupling in an allosteric receptor revealed by mutant cycle analysis. *Biophys J* **96**:3168–3178.

Guitchounts G, Stewart DS, and Forman SA (2012) Two etomidate sites in α1β2γ2 γ-aminobutyric acid type A receptors contribute equally and noncooperatively to modulation of channel gating. *Anesthesiology* **116**:1235–1244.

Harrison NL and Simmonds MA (1984) Modulation of the GABA receptor complex by a steroid anaesthetic. *Brain Res* **323**:287–292.

Hidalgo P and MacKinnon R (1995) Revealing the architecture of a K^+ channel pore through mutant cycles with a peptide inhibitor. *Science* **268**:307–310.

Horovitz A (1996) Double-mutant cycles: a powerful tool for analyzing protein structure and function. *Fold Des* **1**:R121–R126.

Hosie AM, Wilkins ME, da Silva HM, and Smart TG (2006) Endogenous neurosteroids regulate $GABA_A$ receptors through two discrete transmembrane sites. *Nature* **444**:486–489.

Katzenellenbogen JA, Johnson Jr HJ, Carlson KE, and Myers HN (1974) Photoreactivity of some light-sensitive estrogen derivatives. Use of an exchange assay to determine their photointeraction with the rat uterine estrogen binding protein. *Biochemistry* **13**:2986–2994.

Kinde MN, Bu W, Chen Q, Xu Y, Eckenhoff RG, and Tang P (2016) Common anesthetic-binding site for inhibition of pentameric ligand-gated ion channels. *Anesthesiology* **124**:664–673.

Laverty D, Desai R, Uchański T, Masiulis S, Stec WJ, Malinauskas T, Zivanov J, Pardon E, Steyaert J, Miller KW, et al. (2019) Cryo-EM structure of the human α1β3γ2 $GABA_A$ receptor in a lipid bilayer. *Nature* **565**:516–520.

Laverty D, Thomas P, Field M, Andersen OJ, Gold MG, Biggin PC, Gielen M, and Smart TG (2017) Crystal structures of a $GABA_A$-receptor chimera reveal new endogenous neurosteroid-binding sites. *Nat Struct Mol Biol* **24**:977–985.

Li P, Bracamontes J, Katona BW, Covey DF, Steinbach JH, and Akk G (2007a) Natural and enantiomeric etiocholanolone interact with distinct sites on the rat α1β2γ2L $GABA_A$ receptor. *Mol Pharmacol* **71**:1582–1590.

Li P, Shu HJ, Wang C, Mennerick S, Zorumski CF, Covey DF, Steinbach JH, and Akk G (2007b) Neurosteroid migration to intracellular compartments reduces steroid concentration in the membrane and diminishes $GABA_A$ receptor potentiation. *J Physiol* **584**:789–800.

LiCata VJ and Ackers GK (1995) Long-range, small magnitude nonadditivity of mutational effects in proteins. *Biochemistry* **34**:3133–3139.

Marty MT, Baldwin AJ, Marklund EG, Hochberg GK, Benesch JL, and Robinson CV (2015) Bayesian deconvolution of mass and ion mobility spectra: from binary interactions to polydisperse ensembles. *Anal Chem* **87**:4370–4376.

Masiulis S, Desai R, Uchański T, Serna Martin I, Laverty D, Karia D, Malinauskas T, Zivanov J, Pardon E, Kotecha A, et al. (2019) $GABA_A$ receptor signalling mechanisms revealed by structural pharmacology. *Nature* **565**:454–459.

Michel MC, Murphy TJ, and Motulsky HJ (2020) New author guidelines for displaying data and reporting data analysis and statistical methods in experimental biology. *Mol Pharmacol* **97**:49–60.

Miller PS, Scott S, Masiulis S, De Colibus L, Pardon E, Steyaert J, and Aricescu AR (2017) Structural basis for $GABA_A$ receptor potentiation by neurosteroids. *Nat Struct Mol Biol* **24**:986–992.

Monod J, Wyman J, and Changeux JP (1965) On the nature of allosteric transitions: a plausible model. *J Mol Biol* **12**:88–118.

Park-Chung M, Malayev A, Purdy RH, Gibbs TT, and Farb DH (1999) Sulfated and unsulfated steroids modulate γ-aminobutyric acid A receptor function through distinct sites. *Brain Res* **830**:72–87.

Peters JA, Kirkness EF, Callachan H, Lambert JJ, and Turner AJ (1988) Modulation of the $GABA_A$ receptor by depressant barbiturates and pregnane steroids. *Br J Pharmacol* **94**:1257–1269.

Phulera S, Zhu H, Yu J, Claxton DP, Yoder N, Yoshioka C, and Gouaux E (2018) Cryo-EM structure of the benzodiazepine-sensitive $\alpha1\beta1\gamma2S$ tri-heteromeric $GABA_A$ receptor in complex with GABA. *eLife* **7**:e39383.

Schreiber G and Fersht AR (1995) Energetics of protein-protein interactions: analysis of the barnase-barstar interface by single mutations and double mutant cycles. *J Mol Biol* **248**:478–486.

Shin DJ, Germann AL, Johnson AD, Forman SA, Steinbach JH, and Akk G (2018) Propofol is an allosteric agonist with multiple binding sites on concatemeric ternary $GABA_A$ receptors. *Mol Pharmacol* **93**:178–189.

Shin DJ, Germann AL, Steinbach JH, and Akk G (2017) The actions of drug combinations on the $GABA_A$ receptor manifest as curvilinear isoboles of additivity. *Mol Pharmacol* **92**:556–563.

Steinbach JH and Akk G (2019) Applying the Monod-Wyman-Changeux allosteric activation model to pseudo-steady-state responses from $GABA_A$ receptors. *Mol Pharmacol* **95**:106–119.

Sugasawa Y, Bracamontes JR, Krishnan K, Covey DF, Reichert DE, Akk G, Chen Q, Tang P, Evers AS, and Cheng WWL (2019) The molecular determinants of neurosteroid binding in the $GABA_A$ receptor. *J Steroid Biochem Mol Biol* **192**:105383.

Sugasawa Y, Cheng WW, Bracamontes JR, Chen ZW, Wang L, Germann AL, Pierce SR, Senneff TC, Krishnan K, Reichert DE, et al. (2020) Site-specific effects of neurosteroids on $GABA_A$ receptor activation and desensitization. *eLife* **9**:e55331.

Szabo A, Nourmahnad A, Halpin E, and Forman SA (2019) Monod-Wyman-Changeux allosteric shift analysis in mutant $\alpha1\beta3\gamma2L$ $GABA_A$ receptors indicates selectivity and crosstalk among intersubunit transmembrane anesthetic sites. *Mol Pharmacol* **95**:408–417.

Ziemba AM, Szabo A, Pierce DW, Haburcak M, Stern AT, Nourmahnad A, Halpin ES, and Forman SA (2018) Alphaxalone binds in inner transmembrane $\beta+$-$\alpha-$ interfaces of $\alpha1\beta3\gamma2$ γ-aminobutyric acid type A receptors. *Anesthesiology* **128**:338–351.

Address correspondence to: Gustav Akk, Department of Anesthesiology, Washington University School of Medicine, Campus Box 8054, 660 S. Euclid Ave., St. Louis, MO 63110. E-mail: akk@morpheus.wustl.edu

Supplemental information MOLPHARM-AR-2021-000268

Intrasubunit and intersubunit steroid binding sites independently and additively mediate α1β2γ2L $GABA_A$ receptor potentiation by the endogenous neurosteroid allopregnanolone

Allison L. Germann, Spencer R. Pierce, Hiroki Tateiwa, Yusuke Sugasawa, David E. Reichert, Alex S. Evers, Joe Henry Steinbach, and Gustav Akk

Department of Anesthesiology (ALG, SRP, HT, ASE, JHS, GA), Radiology (DER), the Taylor Family Institute for Innovative Psychiatric Research (DER, ASE, JHS, GA), Washington University School of Medicine, St. Louis, MO 63110, and Department of Anesthesiology and Pain Medicine (YS), Juntendo University School of Medicine, Tokyo 113-8421, Japan

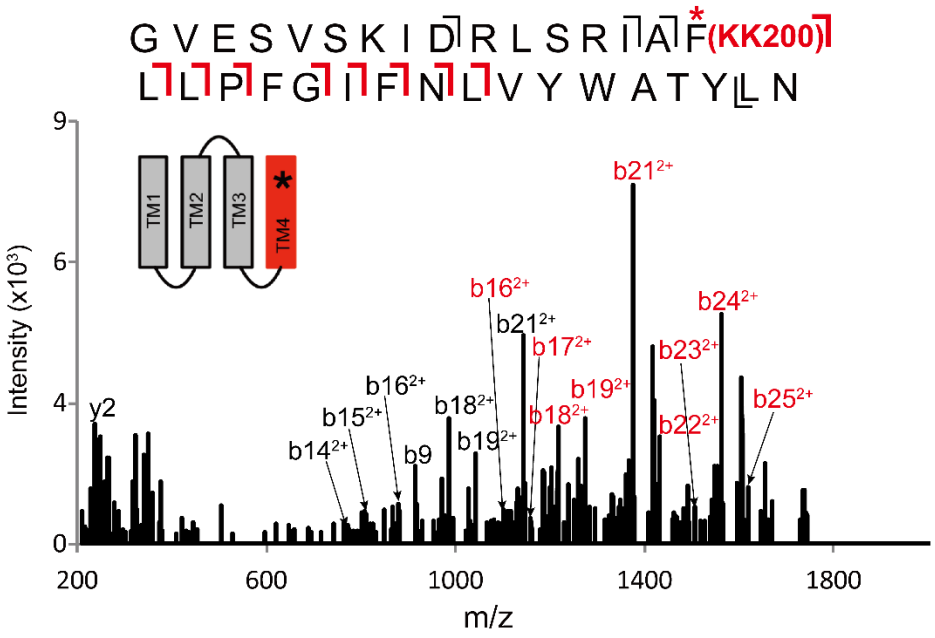

Supplemental Figure 1. A mutation in ELIC-α1 GABA$_A$ receptor alters neurosteroid photolabeling orientation. HCD fragmentation spectrum of the ELIC-α1 GABA$_A$ receptor TM4 tryptic peptide photolabeled with 100 μM KK200 in the V227W mutant. Red and black indicate fragment ions that do or do not contain KK200, respectively. Schematic highlights in red identify the TMD being analyzed and the asterisk denotes the location of KK200.